A Kind of Novel Method of Power Allocation With Limited Cross-Tier Interference for CRN

TING ZHANG[1,2]**, (Member, IEEE), DEGAN ZHANG**[1,2]**, (Member, IEEE), JIANNING QIU**[1,2]**, (Member, IEEE), XIAODAN ZHANG**[3]**, (Member, IEEE), PENGZHEN ZHAO**[1,2]**, (Member, IEEE), AND CHANGLE GONG**[1,2]**, (Member, IEEE)**

[1]Key Laboratory of Computer Vision and System (Tianjin University of Technology), Ministry of Education, Tianjin 300384, China
[2]Tianjin Key Lab of Intelligent Computing and Novel Software Technology, Tianjin University of Technology, Tianjin 300384, China
[3]Institute of Institute of Scientific and Technical Information of China, Beijing 100038, China

Corresponding authors: Degan Zhang (2310674826@qq.com) and Jianning Qiu (1185638995@qq.com)

ABSTRACT A kind of novel method of power allocation with limited cross-tier interference for cognitive radio network (CRN) is proposed in this paper. In this method, an interference-limited power allocation algorithm based on filter bank multi-carrier-offset quadrature amplitude modulation (FBMC-OQAM) is put forward. In order to improve the energy efficiency of the entire network and protect secondary users (SUs) in the network from too much interference, cross-tier interference limit is adopted, at the same time, virtual queue is designed to transform the extra packet delay caused by the contention for the channel of multi-user into the queuing delay. Taking the energy efficiency as the objective function, a nonlinear programming approach with nonlinear constraints is innovatively proposed under the constraints of time delay and transmission power. An iterative algorithm in order to solve the problem is also put forward. In the new algorithm, the fractional objective function is transformed into polynomial form, and the global optimal solution is obtained by iteration after reducing the computational complexity. In addition, a sub-optimal algorithm is proposed to reduce computational complexity. The experimental results show that the optimal algorithm has higher performance while the sub-optimal algorithm has a lower computational complexity. The presented method has very good practical importance for the CRN.

INDEX TERMS Cognitive radio network (CRN), power allocation, FBMC-OQAM, Lagrange dual.

I. INTRODUCTION

The cognitive radio (CR) network (or CRN) [1]–[3] is a wireless communication network composed of cognitive users. Some or all of the devices in a CR network can access authorized as well as unauthorized frequency bands. Thus, compared with traditional wireless networks, CR networks have high spectral efficiency, and this makes them a key technology for next-generation mobile communication networks. The spectrum-sharing cognitive radio network is an interference-controlled CR network that can interfere with the primary user (PU) but cannot exceed its interference temperature limit. An interference temperature limit is added to

The associate editor coordinating the review of this manuscript and approving it for publication was Xianfu Lei.

the transmission power of the secondary user (SU) to ensure that the limit of interference in each PU is not exceeded. The interference temperature limit thus plays an important role in resource allocation for such models. SUs can obtain the interference temperature limit by energy detection or collaboration, where the SUs can directly access the PU network without the real-time perception of the PU. In multi-carrier modulation technology, orthogonal frequency-division multiplexing (OFDM) has been considered as modulation technology for CR networks [4]–[7]. However, when the network encounters asynchronous transmission, the data rate of OFDM can be affected by imperfect timing and frequency synchronization. Asynchronous transmission results in the inter-carrier interference, i.e., interference from one sub-carrier affects adjacent sub-carriers. As an alternative

method of modulation, filter bank multi-carrier (FBMC) modulation [8]–[12] leads to a smaller loss in data transmission rate in asynchronous communication than OFDM because it does not require a cyclic prefix. Moreover, with the offset quadrature-amplitude modulation (OQAM) and poly-phase network, FBMC- OQAM reduces complexity, and has the advantages of insensitivity to an offset in carrier frequency, as well as high energy and spectral efficiency [13]–[20]. In recent years, the scale of users has expanded rapidly, a variety of ubiquitous wireless services have grown quickly, and the energy consumption of battery-powered mobile devices has increased with the continual development of information and communication technologies [21]–[28]. However, owing to the slow development of battery technology and the limitations on battery size, it is challenging to optimize the energy consumption of mobile devices from hardware. Therefore, improving the energy efficiency of wireless networks is important for wireless access in next-generation mobile communication [29]–[35]. Energy-efficient resource allocation has emerged as the cutting-edge technology for the development of network throughput, expansion of the range of wireless network transmission, and an improvement in link reliability [36]–[42]. With the aim of green communication [43]–[46], designing an efficient and accurate resource allocation algorithm is necessary but challenging [47]–[52].

In this paper, we study an energy-efficient power allocation problem in multi-user spectrum-sharing cognitive radio networks with limits on the total rate of data transmission and power consumption [54]–[58]. The main novelty contributions of our work can be summarized as follows:

A kind of novel method of power allocation with limited cross-tier interference for cognitive radio network (CRN) is proposed in this paper. In this new method, we formulate a spectrum-sharing cognitive radio network model with constraints on the total rate of data transmission and power consumption. Considering the heights of the antennas of the base station and secondary users, we present an optimal energy-efficient power allocation algorithm called the EEPA and a sub-optimal energy-efficient power allocation algorithm called the SEEPA. In view of the non-convexity of the original optimization problem, the EEPA converts it into a convex optimization problem, formulates a dual Lagrangian function, and finds the global optimal solution by iteration. The SEEPA delivers performance slightly poorer than that of the EEPA but has lower computational complexity.

The remainder of this paper is organized as follows. Section II introduces research related works, and we describe the proposed multi-user spectrum-sharing cognitive radio network model in Section III. A transformation of the problem is illustrated in Section IV. Section V and section VI design and develop the optimal and sub-optimal energy-efficient power allocation algorithms. The results of experiments to verify the proposed method and a discussion are provided in Section VII, and we give the conclusions of this study in Section VIII.

II. RELATED WORKS

In one of problems of resource allocation, power allocation has been widely used to maximize the throughput of small-cell networks (SCNs) while alleviating cross-tier interference in two-layer networks. Power control was used in [8] to guarantee the signal-to- interference-plus- noise ratio (SINR) of small-cell users (SUs). In [9], a Lagrangian dual decomposition-based power allocation scheme was proposed to reduce cross-tier interference. Channel allocation has also been used to suppress cross-tier interference. A sub-channel allocation method in SCNs was implemented by minimizing the interference of the primary base station (PBS) using the correlated equilibrium game method in [10]. Reference [11] proposed a joint power and sub-channel allocation algorithm to maximize the total throughput of dense SCNs. In [8]–[11], only the performance of the physical layer (in terms of throughput, for instance) was considered while ignoring the arrival and delay requirements of burst data in SUs. To overcome interference, Dang et al. proposed a joint optimal power allocation, relay selection, and sub-carrier allocation scheme in [12]. In [13], sub-carrier pair and power allocation were optimized to maximize the weighted transmission rate of point-to-point OFDM in decode-and-forward (DF) relay networks. Based on perfect self-interference cancellation, [14] proposed an orthogonal frequency-division multiple access (OFDMA) assisted joint resource allocation scheme in a multi-user two-way amplify-and-forward (AF) relay network. In [12]–[15], the optimization of the total transmission rate, power, and sub-carrier allocation in areas with high SINR was key to achieving higher throughput while the balance between energy dissipation in networks and the total rate of data transmission on different links was ignored. In [16], the arrival of burst data and cross-tier interference-sensitive resource management were considered to maximize the throughput of SCNs without performance delay. Li et al. proposed a delay-sensitive resource allocation algorithm based on the Markov decision process to maximize the average delay for all users in [17]. Because the authors focused on the average delay for all users, the method of resource allocation and providing an explicit delay guarantee for users were ignored. In [18], a cross-tier scheduling algorithm for maximizing the time-averaged throughput under delay constraints on users in a single-cell OFDMA network was proposed. However, owing to a lack of cross-tier interference, the algorithm can't be directly applied to spectrum-sharing SCNs. Reference [19] proposed a scheme to jointly control the physical and transport layers that can satisfactorily manage cross-tier interference through resource management in spectrum-sharing SCNs, delay in the SU, and a constraint on cross-tier interference.

This paper investigates the resource allocation problem in FBMC-OQAM-based multiuser spectrum-sharing CR networks. Some of the research related to this problem is in [20]–[29]. The authors of [20] noted that interference suppression is a critical issue in CR networks. The limit on the interference temperature in CR networks was proposed

in [21] to reduce interference from secondary networks to primary networks with the same spectral priority. Interference suppression based on a resource allocation strategy was also studied in wireless cognitive networks. In [22], a dual decomposition method based on sub-channel selection and power allocation was proposed for the limit on the interference temperature as an independent variable in CR networks. In [23] and [24], a joint sub-channel and power allocation method was proposed to maximize system throughput by considering the interference temperature limit on each sub-channel of primary users in multi-cellular cognitive networks. However, the interference temperature can't be directly applied to SCNs because of a lack of cognitive capability of the SU [25]. To solve this problem, the interference temperature limit can be sent to the SCNs via a macro base station [25]–[27]. In all the above studies, the authors didn't use energy efficiency as the target of optimization, but it is an important indicator in wireless communication networks. Energy efficiency has attracted considerable research interest in academia and the industry because it considered to have a significant impact on CR networks [28]–[30]. Many researches have recently focused on energy efficiency and resource allocation [31]–[33]. A dynamic resource allocation algorithm was proposed in [31] based on utility in relay-assisted OFDMA systems for maximizing the average utility of multiple services for all users, but it does not consider energy efficiency. Zarakovitis and Ni proposed a downlink transmission energy-efficient resource allocation scheme in [32] in a multi-user OFDMA network in case of perfect channel state information, and studied the joint sub-carrier and power allocation problem under a total power constraint in multi-user downlink OFDMA networks. The resource allocation problem in [32] optimized only energy efficiency in the downlink scenario without considering multi-user interference in the network, which can inhibit performance, i.e., the performance worsens when the number of mobile user increases. Reference [33]–[36] proposed an energy-efficient power allocation scheme in AF networks. However, when using energy efficiency as the objective function, the joint sub-carrier and power allocation schemes in DF relay networks are identical to those in AF networks. Thus, a joint power and sub-carrier resource allocation scheme was proposed in [37]–[42] in the DF relay interference network. By focusing on CR networks, a non-cooperative SU downlink energy-efficient resource allocation problem was discussed in [43]–[48] using game theory.

The analysis of the above literature shows that most resource allocation algorithms are NP-hard problems, and the optimal algorithms usually have higher complexity while those with lower complexity often involve sacrificing system performance [49]–[54]. Therefore, it is necessary to consider the trade-off between algorithmic complexity and system performance in the design of resource allocation algorithms using convex optimization theory, game theory, graph theory, and other methods [55]–[58].
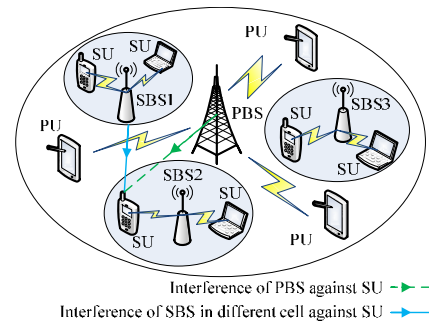

FIGURE 1. System model.

III. PROBLEM FORMULATION&SYSTEM MODELLING

As the spectral access method in this paper does not require considering the communication of the PU, it reduces the time needed to determine its activity through perception and analysis. To improve the efficiency of communication, a scenario featuring a multi-user CR network is considered. As figure 1, the network has L sub-carriers with a total bandwidth of B. A PBS and M SUs are randomly distributed in K cells. Discarding the case involving a diversity of antennas, it is assumed that each transceiver of the PUs and the SUs contains an antenna. The users can realize power control by exchanging information with each other without the collection and processing of complete channel information by the secondary base station (SBS) because of the characteristics of the structure of the network. Under the spectrum-sharing mode used in this paper, the SUs can use the band of the authorized users, and it is necessary to ensure that interference at the receiver of each PU can't exceed the interference temperature limit.

A. TRANSMISSION POWER
Let $P_{k,m,l}$ denote the power distributed to the l-th sub-carrier of the m-th SU in the k-th cell. The total transmission power P_{tot} can then be expressed as

$$P_{tot} = \sum_{k=1}^{K} \sum_{m=1}^{M} \sum_{l=1}^{L} \left(\xi P_{k,m,l} + P_c \right) \qquad (1)$$

where ξ denotes the reciprocal of the drain efficiency of the power amplifier and P_c denotes the power consumed by the circuit.

B. INTERFERENCE TEMPERATURE LIMIT
Medjahdi *et al.* noted that the quantitative interference generated by certain sub-carrier affects the number of adjacent sub-carriers, in [36]. They claimed that such interference generated by FBMC multiple-access technology affects up to three sub-carriers. This paper uses the interference weight vector given in [36] shown in Table 1. Unless otherwise specified, the weight vector is denoted by $V = [V_0, V_1]$.

The interference temperature limit is composed of two parts in this paper: the interference between the sender of the PBS and the receiver of SUs, and that between the sender of SBSs in different cells and the receiver of SUs. The interference between the sender of SBSs in different cells and the

TABLE 1. Interference-weighted vector ($\times 10^{-3}$).

	1	1±1	1±2	1±3	1±4	1±5	1±6	1±7	1±8
FBMC	82.3	88.1	0	0	0	0	0	0	0

receiver of SUs is denoted by

$$I_{SBS} = \sum_{\substack{m'=1 \\ m' \neq m}}^{M} \sum_{\substack{l'=1 \\ l' \neq l}}^{L} P_{k,m',l'} V_{|l-l'|} G_{k,m',l'} \quad (2)$$

where $G_{k',m',l}$ denotes the channel gain between the k-th SBS and the m'-th SU at the l-th sub-carrier. Accordingly, interference between the sender of the PBS and the receiver of SUs is denoted by

$$I_{PBS} = \sum_{l'=1}^{L} P_{k,m,l'} V_{|l-l'|} G_{k,p,l'} \quad (3)$$

where $G_{k,p,l}$ denotes the channel gain between the PBS and the m-th SU in the k-th SBS at the l-th sub-carrier. Overall, the interference temperature limit $I_{k,m,l}$ between the m-th SU and the k-th cell at the l-th sub-carrier is denoted by

$$\begin{aligned} I_{k,m,l} &= I_{SBS} + I_{PBS} \\ &= \sum_{\substack{m'=1 \\ m' \neq m}}^{M} \sum_{\substack{l'=1 \\ l' \neq l}}^{L} P_{k,m',l'} V_{|l-l'|} G_{k,m',l'} \\ &\quad + \sum_{l'=1}^{L} P_{k,m,l'} V_{|l-l'|} G_{k,p,l'} \end{aligned} \quad (4)$$

C. SINR AND TRANSMISSION RATE
We define the SINR $\psi_{k,m,l}$ of the sender of the m-th SU in the k-th cell as

$$\psi_{k,m,l} = \frac{P_{k,m,l} G_{k,m,l}}{N_0 + I_{k,m,l}} \quad (5)$$

where N_0 denotes thermal noise in the sub-carrier, $G_{k,m,l}$ denotes the channel gain between the SBS in the k-th cell and the m-th SU at the l-th sub-carrier. According to Shannon's theorem, the total data transmission rate R_{tot} can be expressed as

$$\begin{aligned} R_{tot} &= \sum_{k=1}^{K} \sum_{m=1}^{M} \sum_{l=1}^{L} \frac{B}{L} \log_2 \left(1 + \psi_{k,m,l}\right) \\ &= \sum_{k=1}^{K} \sum_{m=1}^{M} \sum_{l=1}^{L} \frac{B}{L} \log_2 \left(1 + \frac{P_{k,m,l} G_{k,m,l}}{N_0 + I_{k,m,l}}\right) \end{aligned} \quad (6)$$

where B/L denotes the transmission bandwidth in the sub-carrier.

D. BER
In the FBMC-OQAM system, we consider a method of modulation that uses the M-QAM signal constellation. For the given SINR $\psi_{k,m,l}$ of the sender of the m-th SU in the k-th cell, the mean BER $E_{k,m,l}$ can be written as follows [37]:

$$\mathcal{E}_{k,m,l} = 0.2\exp\left[-\frac{1.5 P_{k,m,l} G_{k,m,l}}{(M-1)\left(N_0 + I_{k,m,l}\right)}\right] \quad (7)$$

where M denotes the number of points in each signal constellation.

E. DELAY
The concept of a virtual queue is introduced to measure the interaction between users. Assume that channel F_k in each cell corresponds to a virtual queue $\widetilde{Q}_k$. The packets assigned and transmitted on channel F_k in entire cells enter into virtual queue $\widetilde{Q}_k$ corresponding to channel F_k after being queued in the physical queue. After queuing in the virtual queue $\widetilde{Q}_k$, the packets can be sent on channel F_k.

According to the concept of the virtual queue, the extra packet delay caused by the contention for channel F_k among multiple users in the MAC protocol is transformed into queuing delay $\widetilde{W}_k$ in virtual queue $\widetilde{Q}_k$ corresponding to channel F_k. Thus, it can be calculated by queuing theory. Finally, the packet service time of physical queue Q_{jk} is corrected to the sum of the packet transmission time and the queuing time of the virtual queue. The input packet stream of the virtual queue is the superposition of the transmission rates of all users distributed on channel F_k, which can be considered a Poisson process:

$$\widetilde{R}_k = \sum_{m=1}^{M} R_{k,m} \quad (8)$$

The virtual queue $\widetilde{Q}_k$ is a logical concept that does not exist physically. Groupings in $\widetilde{Q}_k$ are physically dispersed in each SU. The service time of the virtual queue is the packet transmission time while the packet processing rate of the server is the packet sending time of each SU on channel F_k. Although the packet in $\widetilde{Q}_k$ is transmitted by a different transmitter of the SU, only one transmitter can access the channel corresponding to $\widetilde{Q}_k$, i.e., there is only one variable rate (service capability) server in $\widetilde{Q}_k$.

In the M/G/1 queuing system, it is assumed that the service time of the m-th SU in the k-th cell at the l-th sub-carrier is expressed as $X_{k,m,l}$. $X_{k,m,l}$ is independent and identically distributed in the arrival interval. The mean and second moments of service time in the k-th cell are expressed as

Mean service time:

$$\overline{X}_k = \left(E\left[X_{1,m,l}\right], E\left[X_{2,m,l}\right], \cdots, E\left[X_{K,m,l}\right]\right)^{\mathrm{T}}$$

Second moment of service time:

$$\overline{X_k^2} = \left(E\left[X_{1,m,l}^2\right], E\left[X_{2,m,l}^2\right], \cdots, E\left[X_{K,m,l}^2\right]\right)^{\mathrm{T}}$$

According to the P-K formula, the average waiting time in a cell for an M/G/1 queuing system is as

$$W_k = \frac{\widetilde{R}_k \overline{X_k^2}}{2\left(1 - \widetilde{R}_k \overline{X}_k\right)} \quad (9)$$

The average delay in a cell is obtained by the P-K formula as

$$T_k = \overline{X}_k + W_k = \overline{X}_k + \frac{\widetilde{R}_k \overline{X_k^2}}{2\left(1 - \widetilde{R}_k \overline{X}_k\right)} \quad (10)$$

where $\widetilde{R}_k \overline{X}_k$ denotes the ratio of arrival rate to service rate reflecting how busy the system is. When $\widetilde{R}_k \overline{X}_k$ increases, the number of users increases in the steady state of the system. When $\widetilde{R}_k \overline{X}_k$ tends to one, the number of users tends to infinity in the steady state of the system. When $\widetilde{R}_k \overline{X}_k > 1$, there is not enough time for the system to service, and the number of users inevitably becomes infinite.

The power allocation problem in this paper can be considered a nonlinear programming problem with nonlinear constraints as

$$
\begin{aligned}
\max \; EE\left(P_{k,m,l}\right) &= \frac{R_{tot}}{P_{tot}} \\
&= \frac{\sum_{k=1}^{K}\sum_{m=1}^{M}\sum_{l=1}^{L} \frac{B}{L}\log_2\left(1 + \frac{P_{k,m,l}G_{k,m,l}}{N_0 + I_{k,m,l}}\right)}{\sum_{k=1}^{K}\sum_{m=1}^{M}\sum_{l=1}^{L}\left(\xi P_{k,m,l} + P_c\right)}
\end{aligned}
$$

$$
\text{s.t. } (C1) \sum_{k=1}^{K}\sum_{m=1}^{M}\sum_{l=1}^{L}\left(\xi P_{k,m,l} + P_c\right) \leq P_{tot}^{\max}
$$

$$
(C2) \; \overline{X}_k + \frac{\widetilde{R}_k \overline{X}_k^2}{2\left(1 - \widetilde{R}_k \overline{X}_k\right)} \leq T_k^{\text{th}}
$$

$$
(C3) \; E_{k,m,l} \leq E^{\text{th}}
$$

$$
(C4) \; I_{k,m,l} \leq I^{\text{th}} \tag{11}
$$

Because the Hessian matrix of the objective function is not a positive-semidefinite matrix, the objective function is non-convex and can't be solved by convex optimization. The power allocation problem (11) is transformed in the next section.

IV. TRANSFORMATION FOR NONCONVEX PROBLEM

The objective function of the optimization problem as equation (11) is non-convex. Thus, the optimization problem as equation (11) is also a non-convex optimization problem. There is no standard way to solve this problem, because of which the objective function needs to be transformed. The molecular part of the objective function $\sum_{k=1}^{K}\sum_{m=1}^{M}\sum_{l=1}^{L}(B/L)\log_2(1 + P_{k,m,l}G_{k,m,l}/(N_0 + I_{k,m,l}))$ is concave while the denominator $\sum_{k=1}^{K}\sum_{m=1}^{M}\sum_{l=1}^{L}(\xi P_{k,m,l} + P_c)$ has no concavity or convexity. The target is to change the objective function into a concave function over the convex function. Thus, the denominator needs to be processed. Let $\widehat{P}_{k,m,l} = \ln P_{k,m,l}$, i.e., replace $P_{k,m,l}$ with $e^{\widehat{P}_{k,m,l}}$. Then, the optimization problem (11) can be rewritten as

$$
\begin{aligned}
\max \; EE\left(\widehat{P}_{k,m,l}\right) \\
= \frac{\sum_{k=1}^{K}\sum_{m=1}^{M}\sum_{l=1}^{L} \frac{B}{L}\log_2\left(1 + \frac{e^{\widehat{P}_{k,m,l}}G_{k,m,l}}{N_0 + \widehat{I}_{k,m,l}}\right)}{\sum_{k=1}^{K}\sum_{m=1}^{M}\sum_{l=1}^{L}\left(\xi e^{\widehat{P}_{k,m,l}} + P_c\right)}
\end{aligned}
$$

$$
\text{s.t. } (C1) \sum_{k=1}^{K}\sum_{m=1}^{M}\sum_{l=1}^{L}\left(\xi e^{\widehat{P}_{k,m,l}} + P_c\right) \leq P_{tot}^{\max}
$$

$$
(C2) \sum_{m=1}^{M}\sum_{l=1}^{L} \frac{B}{L}\log_2\left(1 + \frac{e^{\widehat{P}_{k,m,l}}G_{k,m,l}}{N_0 + \widehat{I}_{k,m,l}}\right)
$$

$$
\leq \frac{2\left(T_k^{\text{th}} - \overline{X}_k\right)}{2\left(T_k^{\text{th}} - \overline{X}_k\right)\overline{X}_k + \overline{X}_k^2}
$$

$$
(C3) \; \widehat{\mathcal{E}}_{k,m,l} = 0.2\exp\left[-\frac{1.5 e^{\widehat{P}_{k,m,l}}G_{k,m,l}}{(\mathcal{M} - 1)\left(N_0 + \widehat{I}_{k,m,l}\right)}\right]
$$

$$
\leq \mathcal{E}^{\text{th}}
$$

$$
(C4) \; \widehat{I}_{k,m,l} = \sum_{\substack{m'=1 \\ m'\neq m}}^{M}\sum_{\substack{l'=1 \\ l'\nmid}}^{L} e^{\widehat{P}_{k,m',l'}} V_{|l-l'|} G_{k,m',l'}
$$

$$
+ \sum_{l'=1}^{L} e^{\widehat{P}_{k,m,l'}} V_{|l-l'|} G_{k,p,l'} \leq I^{\text{th}} \tag{12}
$$

By means of the transformation, the objective function of the original problem (11) is transformed into a concave function over a convex function form as shown in the equation (12). In the next section, the fractional form of the objective function is transformed into its equivalent polynomial form, and the optimal solution of the problem is obtained by the iterative method.

V. DESIGNED OF ENERGY-EFFICIENT POWER ALLOCATION ALGORITHM

Because of the fractional form of the optimization problem as equation (12), the solution process is very complex. We thus use the Dinkelbach method [35] to transform it into polynomial form. Thus, the nonlinear fractional programming problem $\max\left\{R_{tot}/P_{tot}\right\}$ can be transformed into $\max\left\{R_{tot} - \gamma P_{tot}\right\}$. The optimization problem as equation (12) can be expressed as equation (13):

$$
\begin{aligned}
\max \; & f_{EE}\left(\gamma, \widehat{P}_{k,m,l}\right) \\
&= \sum_{k=1}^{K}\sum_{m=1}^{M}\sum_{l=1}^{L} \frac{B}{L}\log_2\left(1 + \frac{e^{\widehat{P}_{k,m,l}}G_{k,m,l}}{N_0 + \widehat{I}_{k,m,l}}\right) \\
&\quad - \gamma \cdot \sum_{k=1}^{K}\sum_{m=1}^{M}\sum_{l=1}^{L}\left(\xi e^{\widehat{P}_{k,m,l}} + P_c\right)
\end{aligned}
$$

$$
\text{s.t. } (C1), (C2), (C3), (C4) \tag{13}
$$

Lemma 1: $F(\gamma) = \max\left\{R_{tot}(P) - \gamma P_{tot}(P)\middle| P \in S\right\}$ is convex over E^1.

Proof: Let p_t maximize $F(t\gamma' + (1-t)\gamma'')$ with $\gamma' \neq \gamma''$ and $0 \leq t \leq 1$. Then,

$$
\begin{aligned}
& F\left(t\gamma' + (1+t)\gamma''\right) \\
&= R_{tot}(p_t) - \left(t\gamma' + (1-t)\gamma''\right)P_{tot}(p_t) \\
&= t\left[R_{tot}(p_t) - \gamma' P_{tot}(p_t)\right] + (1-t)\left[R_{tot}(p_t) - \gamma'' P_{tot}(p_t)\right] \\
&\leq t \cdot \max\left\{R_{tot}(p) - \gamma' P_{tot}(p)\middle| p \in S\right\} \\
&\quad + (1-t) \cdot \max\left\{R_{tot}(p) - \gamma'' P_{tot}(p)\middle| p \in S\right\} \\
&= tF(\gamma') + (1-t)F(\gamma'') \tag{14}
\end{aligned}
$$

Lemma 2: $F(\gamma) = \max\left\{R_{tot}(P) - \gamma P_{tot}(P)\middle| P \in S\right\}$ is strictly monotonically decreasing, i.e., $F(\gamma'') < F(\gamma')$, if $\gamma' < \gamma''$, $\gamma', \gamma'' \in E^1$.

Proof: Let p'' maximize $F(\gamma'')$. Then,

$$
\begin{aligned}
& F(\gamma'') \\
&= \max\left\{R_{tot}(p) - \gamma'' P_{tot}(p)\middle| p \in S\right\} \\
&= R_{tot}(p'') - \gamma'' P_{tot}(p'') < R_{tot}(p'') - \gamma' P_{tot}(p'') \\
&\leq \max\left\{R_{tot}(p) - \gamma' P_{tot}(p)\middle| p \in S\right\} = F(\gamma') \tag{15}
\end{aligned}
$$

Lemma 3: $F(\gamma) = 0$ has a unique solution, γ_0.

Proof: Lemma 3 results from *Lemma 2*, and we have the following fact: $F(\gamma) = +\infty$ and $F(\gamma) = -\infty$.

Lemma 4: Let $P^+ \in S$ and $\gamma^+ = R_{tot}(P^+)/P_{tot}(P^+)$. Then, $F(\gamma^+) \geq 0$.

Proof: $F(\gamma^+) = \max\{R_{tot}(p) - \gamma^+ P_{tot}(p) \mid p \in S\} \geq R_{tot}(p^+) - \gamma^+ P_{tot}(p^+) = 0$. Hence, $F(\gamma^+) \geq 0$.

Proposition 1: $\gamma_0 = R_{tot}(P_0)/P_{tot}(P_0) = \max\{R_{tot}(P)/P_{tot}(P) \mid P \in S\}$, if and only if $F(\gamma_0) = F(\gamma_0, P_0) = \max\{R_{tot}(P) - \gamma_0 P_{tot}(P) \mid P \in S\}$.

Proof: a) Let p_0 be a solution to the problem $\max\{R_{tot}/P_{tot}\}$. For all $p \in S$. We then have

$$\gamma_0 = \frac{R_{tot}(p_0)}{P_{tot}(p_0)} \geq \frac{R_{tot}(p)}{P_{tot}(p)} \tag{16}$$

Thus,

$(\alpha) R_{tot}(p) - \gamma_0 P_{tot}(p) \leq 0$ for all $p \in S$.
$(\beta) R_{tot}(p_0) - \gamma_0 P_{tot}(p_0) = 0$.

From (α), $F(\gamma_0) = \max\{R_{tot}(p) - \gamma_0 P_{tot}(p) \mid p \in S\} = 0$. From (β), we get the maximum, for example, at p_0. Thus, the first part of the proof is complete.

b) Let p_0 be a solution to the problem $\max\{R_{tot} - \gamma P_{tot}\}$ such that $R_{tot}(p_0) - \gamma_0 P_{tot}(p_0) = 0$. The definition of $\max\{R_{tot} - \gamma P_{tot}\}$ implies that for all $p \in S$, we have

$$R_{tot}(p) - \gamma_0 P_{tpt}(p) \leq R_{tot}(p_0) - \gamma_0 P_{tot}(p_0) = 0 \tag{17}$$

Thus,

$(\alpha) R_{tot}(p) - \gamma_0 P_{tot}(p) \leq 0$ for all $p \in S$.
$(\beta) R_{tot}(p_0) - \gamma_0 P_{tot}(p_0) = 0$.

From (α), $\gamma_0 \geq R_{tot}(p)/P_{tot}(p)$ for all $p \in S$, i.e., γ_0 is the maximum value of problem $\max\{R_{tot}/P_{tot}\}$. From (β), we have $\gamma_0 = R_{tot}(p_0)/P_{tot}(p_0)$, i.e., p_0 is a solution vector of problem $\max\{R_{tot}/P_{tot}\}$.

According to the convex optimization theory, the Lagrange multipliers λ_1 and λ_2 are introduced to establish the Lagrange function of the optimization problem as equation (13):

$$
\begin{aligned}
&L\left(\gamma, \widehat{P}_{k,m,l}, \lambda_1, \lambda_2\right) \\
&= f_{EE}\left(\gamma, \widehat{P}_{k,m,l}\right) \\
&\quad - \lambda_1 \left(\sum_{k=1}^{K}\sum_{m=1}^{M}\sum_{l=1}^{L}\left(\xi e^{\widehat{P}_{k,m,l}} + P_c\right) - P_{tot}^{\max}\right) \\
&\quad - \lambda_2 \left(\sum_{m=1}^{M}\sum_{l=1}^{L}\frac{B}{L}\log_2\left(1 + \frac{e^{\widehat{P}_{k,m,l}}G_{k,m,l}}{N_0 + \widehat{I}_{k,m,l}}\right)\right. \\
&\qquad \left. - \frac{2\left(T_k^{th} - \overline{X_k}\right)}{2\left(T_k^{th} - \overline{X_k}\right)\overline{X_k} + \overline{X_k^2}}\right) \Bigg| \begin{matrix} \widehat{I}_{k,m,l} \leq I^{th} \\ E_{k,m,l} \leq E^{th} \\ \lambda_1, \lambda_2 \geq 0 \end{matrix} \tag{18}
\end{aligned}
$$

If we search for the optimal solution by traversal, we can find the theoretical solution such that the computational complexity is too high. Thus, the dual Lagrange method is adopted, and the Lagrange dual function can be expressed as follows:

$$D(\lambda_1, \lambda_2) \triangleq \max_{\gamma, \widehat{P}_{k,m,l}} L\left(\gamma, \widehat{P}_{k,m,l}, \lambda_1, \lambda_2\right)$$
$$s.t. \ (C1), (C2) \tag{19}$$

Definition 1: The optimal solution of optimization problem as equation (13) is denoted by *OP* while the optimal solution of its dual problem is denoted by *DOP*. The difference between the optimal solutions of the optimization problem and its dual are defined as the duality gap *DG*, i.e., $DG = OP\text{-}DOP$.

The duality gap represents the difference between the optimal solution of the original problem and that of the dual problem. If the duality gap is zero, the solution to the original problem can be obtained by solving it such that it has relatively low computational complexity. The duality gap of the optimization problem as equation (13) will be proved to be zero.

Theorem 1: The duality gap *DG* tends to zero, i.e., $DG = OP\text{-}DOP \approx 0$.

Proof: The constraints (C1) - (C4) of the problem as equation (13) can be rewritten as follows:

$$
\begin{aligned}
&\max f_{EE}\left(\gamma, \widehat{P}_{k,m,l}\right) \\
&= \sum_{k=1}^{K}\sum_{m=1}^{M}\sum_{l=1}^{L}\frac{B}{L}\log_2\left(1 + \frac{e^{\widehat{P}_{k,m,l}}G_{k,m,l}}{N_0 + \widehat{I}_{k,m,l}}\right) \\
&\quad - \gamma \cdot \sum_{k=1}^{K}\sum_{m=1}^{M}\sum_{l=1}^{L}\left(\xi e^{\widehat{P}_{k,m,l}} + P_c\right) \\
&s.t. \ C^{(n)}\left(\gamma, \widehat{P}_{k,m,l}\right) \leq \Gamma^{(n)}, \quad n = 1, 2, 3, 4 \tag{20}
\end{aligned}
$$

From [39], it is evident that the duality gap tends to zero, i.e., $DG \approx 0$, when the time-sharing condition is satisfied. We now define the time-sharing property as follows:

Definition 2: Let $\left(\gamma_X^*, \widehat{P}_{k,m,l_X}^*\right)$ and $\left(\gamma_Y^*, \widehat{P}_{k,m,l_Y}^*\right)$ be optimal solutions to the optimization problem as equation (20) with $\Gamma^{(n)} = \Gamma_X$ and $\Gamma^{(n)} = \Gamma_Y$, respectively. Optimization problem as equation (20) is said to satisfy the time-sharing condition if, for any Γ_X, Γ_Y and $0 \leq \theta \leq 1$, there always exists a feasible solution $\left(\gamma_Z, \widehat{P}_{k,m,l_Z}\right)$, such that

$$C^{(n)}\left(\gamma_Z, \widehat{P}_{k,m,l_Z}\right) \leq \theta \cdot \Gamma_X + (1-\theta) \cdot \Gamma_Y \tag{21}$$
$$
\begin{aligned}
f_{EE}\left(\gamma_Z, \widehat{P}_{k,m,l_Z}\right) &\geq \theta f_{EE}\left(\gamma_X^*, \widehat{P}_{k,m,l_X}^*\right) \\
&\quad + (1-\theta) f_{EE}\left(\gamma_Y^*, \widehat{P}_{k,m,l_Y}^*\right) \tag{22}
\end{aligned}
$$

The time-sharing condition can be understood as the maximum of the optimization problem as equation (20) as a function of constraint Γ. A higher Γ implies looser constraints. Roughly speaking, the maximum value of the solution to optimization problem as equation (20) is a monotonically increasing function of Γ. The time-sharing condition means that the maximum value of the optimization problem is a concave function of Γ. Thus, if the maximum value of the optimization problem is a concave function of Γ, $DG \approx 0$.

Let Γ_X, Γ_Y, and Γ_Z be constraint vectors and $\Gamma_Z = \theta \cdot \Gamma_X + (1-\theta) \cdot \Gamma_Y$ for $0 \leq \theta \leq 1$. Let $\left(\gamma_X^*, \widehat{P}_{k,m,l_X}^*\right)$, $\left(\gamma_Y^*, \widehat{P}_{k,m,l_Y}^*\right)$, and $\left(\gamma_Z^*, \widehat{P}_{k,m,l_Z}^*\right)$ be the optimal solutions of optimization

problem as equation (20) under constraints Γ_X, Γ_Y, and Γ_Z, separately. Concavity follows from the definition of the time-sharing condition, i.e., when $\Gamma_Z = \theta \cdot \Gamma_X + (1-\theta) \cdot \Gamma_Y$, the time-sharing condition indicates that the existence of $\left(\gamma_Z^*, \widehat{P}_{k,m,l_Z}^*\right)$ makes

$$C^{(n)}\left(\gamma_Z, \widehat{P}_{k,m,l_Z}\right) \leq \theta \cdot \Gamma_X + (1-\theta) \cdot \Gamma_Y \quad (23)$$

and

$$f_{EE}\left(\gamma_Z, \widehat{P}_{k,m,l_Z}\right) \geq \theta f_{EE}\left(\gamma_X^*, \widehat{P}_{k,m,l_X}^*\right)$$
$$+ (1-\theta) f_{EE}\left(\gamma_Y^*, \widehat{P}_{k,m,l_Y}^*\right) \quad (24)$$

Because $\left(\gamma_Z^*, \widehat{P}_{k,m,l_Z}^*\right)$ is a feasible solution of the optimization problem,

$$f_{EE}\left(\gamma_Z^*, \widehat{P}_{k,m,l_Z}^*\right)$$
$$\geq f_{EE}\left(\gamma_Z, \widehat{P}_{k,m,l_Z}\right)$$
$$\geq \theta f_{EE}\left(\gamma_X^*, \widehat{P}_{k,m,l_X}^*\right) + (1-\theta) f_{EE}\left(\gamma_Y^*, \widehat{P}_{k,m,l_Y}^*\right) \quad (25)$$

Thus, Theorem 1 is proved.

The optimization function of the Lagrangian dual function can be expressed as

$$G(\lambda_1, \lambda_2,) = \min_{\lambda_1,\lambda_2 \geq 0} D(\lambda_1, \lambda_2)$$
$$= \min_{\lambda_1,\lambda_2 \geq 0} \max_{\gamma, \widehat{P}_{k,m,l}} L(\gamma, \widehat{P}_{k,m,l}, \lambda_1, \lambda_2)$$
$$s.t. \ (C1), (C2) \quad (26)$$

We fix λ_1 and find the vector λ_2 that leads to the smallest L. For vector λ_2, the dual function is a convex function such that it can be obtained by multidimensional search. However, the dual function is not necessarily derivable. Thus a sub-gradient algorithm is used instead of the gradient algorithm in this paper. We find the value of λ_1 after finding the minimum value of L. To render the total power fully allocated, the search for λ_1 is based on the sub-gradient algorithm while the corresponding power $\widehat{P}_{k,m,l}$ of each SU is the optimal solution to the problem.

By taking the partial derivative of the Lagrange function with respect to $\widehat{P}_{k,m,l}$ and equating the result to zero, we can get the update equation in the $(t+1)$-th iteration of $\widehat{P}_{k,m,l}$ as

$$P_{k,m,l}(t+1) = \left[\frac{1}{2}\ln\left(\frac{(1-\lambda_2)B}{L\ln 2(\gamma+\lambda_1)\xi} - \frac{N_0+\widehat{I}_{k,m,l}}{G_{k,m,l}}\right)\right]^+ \quad (27)$$

After finding the optimal value of $\widehat{P}_{k,m,l}$, say $\widehat{P}_{k,m,l}^*$, the dual function can be rewritten as

$$D(\lambda_1, \lambda_2) \triangleq \max_{\gamma, P_{k,m,l}^*} L\left(\gamma, \widehat{P}_{k,m,l}^* \lambda_1, \lambda_2\right)$$
$$s.t. \ (C1), (C2) \quad (28)$$

Algorithm 1 Optimal Energy-Efficient Power Allocation

1	Initialize γ, δ and $Ite1$
2	**Repeat**
3	Initialize $\lambda_1^{\max}$, $\lambda_1^{\min}$ and τ
4	**Repeat**
5	Let $\lambda_1 = \left(\lambda_1^{\max} + \lambda_1^{\min}\right)/2$
6	Initialize λ_2, α_2, ε and $Ite2$
7	**Repeat**
8	Update $\widehat{P}_{k,m,l}$ using equation (27)
9	Update λ_2 using equation (29)
10	$Ite2 \leftarrow Ite2 + 1$
11	**Until** $\lvert \lambda_2 \cdot (C2) \rvert < \varepsilon$
12	If $P_{tot} > P_{tot}^{\max}$, $\lambda_1^{\min} = \lambda_1$; else $\lambda_1^{\max} = \lambda_1$
13	**Until** $\lambda_1^{\max} - \lambda_1^{\min} \leq \tau$
14	Update γ using equation (30)
15	$Ite1 \leftarrow Ite1 + 1$
16	**Until** $G_{Ite1} < \delta$ **or** $Ite1 = Ite1_{\max}$

The variable λ_2 of the dual function in the $(t+1)$-th iteration can be updated by following update equation using the sub-gradient algorithm in convex optimization.

$$\lambda_2(t+1)$$
$$= \left[\lambda_2(t) + \alpha_2(t)\left(\sum_{m=1}^{M}\sum_{l=1}^{L}\frac{B}{L}\log_2\right.\right.$$
$$\left.\left.\times \left(1 + \frac{e^{\widehat{P}_{k,m,l}^*(t)}G_{k,m,l}}{N_0 + \widehat{I}_{k,m,l}}\right) - \frac{2\left(T_k^{th} - \overline{X_k}\right)}{2\left(T_k^{th} - \overline{X_k}\right)\overline{X_k} + \overline{X_k^2}}\right)\right]^+ \quad (29)$$

where α_2 is a positive step size.

The equation to update γ the in $(t+1)$-th iteration is expressed as

$$\gamma(t+1) = \frac{\sum_{k=1}^{K}\sum_{m=1}^{M}\sum_{l=1}^{L}\frac{B}{L}\log_2\left(1 + \frac{e^{\widehat{P}_{k,m,l}^*(t)}G_{k,m,l}}{N_0 \widehat{I}_{k,m,l}}\right)}{\sum_{k=1}^{K}\sum_{m=1}^{M}\sum_{l=1}^{L}\left(\xi e^{\widehat{P}_{k,m,l}^*(t)} + P_c\right)} \quad (30)$$

$R_{tot}(P)$ is concave, $P_{tot}(P)$ is convex, and the set of S is convex for all $P \in S$. Because of the continuity of $F(\gamma) = \max\{R_{tot}(P) - \gamma P_{tot}(P) \mid P \in S\}$, the following expression is formulated:

Find P_n and $\gamma_n = R_{tot}(P_n)/P_{tot}(P_n)$, such that
$F(\gamma_n) - F(\gamma_0) = F(\gamma_n) < \delta$ for any given $\delta > 0$.

Moreover, $F(0) = \max\{R_{tot}(P) \mid P \in S\}$. Thus, the algorithm starts at $\gamma = 0$. The energy-efficient power allocation algorithm developed in this paper is shown in Algorithm 1. We first initialize γ, δ, $\lambda_1^{\max}$, $\lambda_1^{\min}$, λ_2, α_2, $Ite1$, and $Ite2$. For given values of γ, λ_1, and λ_2, $\widehat{P}_{k,m,l}$ is updated through equation (27). Then, λ_2 is updated through equation (29) using the updated $\widehat{P}_{k,m,l}$. The iteration of the inner loop has

the following condition:

$$\left| \lambda_2 \cdot \left(\sum_{m=1}^{M} \sum_{l=1}^{L} \frac{B}{L} \log_2 \left(1 + \frac{e^{\widehat{P}_{k,m,l}} G_{k,m,l}}{N_0 + \widehat{I}_{k,m,l}} \right) \right. \right.$$

$$\left. \left. - \frac{2\left(T_k^{\text{th}} - \overline{X_k}\right)}{2\left(T_k^{\text{th}} - \overline{X_k}\right)\overline{X_k} + \overline{X_k^2}} \right) \right| = |\lambda_2 \cdot (C2)| < \varepsilon \quad (31)$$

When the iteration satisfies the condition above, λ_1 can be searched by binary search based on the sub-gradient algorithm. After finding the optimal λ_1, λ_2, and $\widehat{P}_{k,m,l}$, γ can be updated by equation (30). The outer loop ends when it satisfies the condition $G_{Ite1} < \delta$ or reaches the maximum number of iterations.

## VI. DESIGNED OF SUB-OPTIMAL ENERGY-EFFICIENT POWER ALLOCATION ALGORITHM

Because of the high computational complexity of the EEPA algorithm, the performance of some applications with high instantaneous demand is affected. Thus, based on the original EEPA algorithm, a sub-optimal energy-efficient power allocation (SEEPA) algorithm with lower computational complexity is designed in this paper. Although the sub-optimal algorithm reduces computational complexity, it also reduces computational accuracy. The biggest difference between the EEPA and the SEEPA is that an auxiliary variable $\Psi_{k,m,l} \in \left(0, \psi_{k,m,l} \right]$ is introduced in the latter to indicate that the SINR of no SU in the network is lower than a certain vector $\Psi_{k,m,l}$. Thus, problem as equation (13) can be rewritten as

$$\max EE\left(\Psi_{k,m,l}, \widehat{P}_{k,m,l} \right)$$

$$= \frac{\sum_{k=1}^{K} \sum_{m=1}^{M} \sum_{l=1}^{L} \frac{B}{L} \log_2 \left(1 + \Psi_{k,m,l} \right)}{\sum_{k=1}^{K} \sum_{m=1}^{M} \sum_{l=1}^{L} \left(\xi e^{\widehat{P}_{k,m,l}} + P_c \right)}$$

$$s.t. \ (C1) \sum_{k=1}^{K} \sum_{m=1}^{M} \sum_{l=1}^{L} \left(\xi e^{\widehat{P}_{k,m,l}} + P_c \right) \le P_{tot}^{\max}$$

$$(C2) \sum_{m=1}^{M} \sum_{l=1}^{L} \frac{B}{L} \log_2 \left(1 + \Psi_{k,m,l} \right)$$

$$\le \frac{2\left(T_k^{\text{th}} - \overline{X_k}\right)}{2\left(T_k^{\text{th}} - \overline{X_k}\right)\overline{X_k} + \overline{X_k^2}}$$

$$(C3) \ \Psi_{k,m,l} e^{-\widehat{P}_{k,m,l}} \frac{N_0 + \widehat{I}_{k,m,l}}{G_{k,m,l}} \le 1$$

$$(C4) \ \widehat{\mathcal{E}}_{k,m,l} \le \mathcal{E}^{\text{th}}$$

$$(C5) \ \widehat{I}_{k,m,l} \le I^{\text{th}} \quad (32)$$

According to convex optimization theory, the Lagrange multipliers λ_1, λ_2, and λ_3 are introduced to establish the Lagrange function and the optimization function of the dual Lagrangian function of problem as equation (32) as follows:

$$L\left(\Psi_{k,m,l}, \gamma, \widehat{P}_{k,m,l}, \lambda_1, \lambda_2, \lambda_3 \right)$$

$$= f_{EE_m}\left(\Psi_{k,m,l}, \gamma, \widehat{P}_{k,m,l} \right)$$

$$- \lambda_1 \left(\sum_{k=1}^{K} \sum_{m=1}^{M} \sum_{l=1}^{L} \left(\xi e^{\widehat{P}_{k,m,l}} + P_c \right) - P_{tot}^{\max} \right)$$

$$- \lambda_2 \left(\sum_{m=1}^{M} \sum_{l=1}^{L} \frac{B}{L} \log_2 \left(1 + \Psi_{k,m,l} \right) \right.$$

$$\left. - \frac{2\left(T_k^{\text{th}} - \overline{X_k}\right)}{2\left(T_k^{\text{th}} - \overline{X_k}\right)\overline{X_k} + \overline{X_k^2}} \right)$$

$$\left. - \lambda_3 \left(\Psi_{k,m,l} e^{-\widehat{P}_{k,m,l}} \frac{N_0 + \widehat{I}_{k,m,l}}{G_{k,m,l}} - 1 \right) \right| \begin{array}{l} \widehat{I}_{k,m,l} \le I^{\text{th}} \\ \widehat{\mathcal{E}}_{k,m,l} \le \mathcal{E}^{\text{th}} \\ \lambda_1, \lambda_2, \lambda_3, \ge 0 \end{array} \quad (33)$$

$$G(\lambda_1, \lambda_2, \lambda_3)$$

$$= \min_{\lambda_1, \lambda_2, \lambda_3 \ge 0} D\left(\lambda_1, \lambda_2, \lambda_3 \right)$$

$$\triangleq \min_{\lambda_1, \lambda_2, \lambda_3 \ge 0} \max_{\Psi_{k,m,l}, \gamma, \overline{P}_{k,m,l}} L\left(\Psi_{k,m,l}, \gamma, \widehat{P}_{k,m,l}, \lambda_1, \lambda_2, \lambda_3 \right)$$

$$s.t. \ (C1), (C2), (C3) \quad (34)$$

According to the aforementioned equation (27) and the equation (33), we can deduce (the reason is as the equation (27) and the equation (33)) that by taking the partial derivative of the Lagrange function with respect to $\widehat{P}_{k,m,l}$ and $\Psi_{k,m,l}$, and equating the result to zero, we can get the update equation in the $(t+1)$-th iteration of $\widehat{P}_{k,m,l}$ and $\Psi_{k,m,l}$ as the equation (35) and the equation (36) which has the similar form and meaning to the equation (27):

$$P_{k,m,l}(t+1) = \left[\frac{1}{2} \ln \left(\frac{\lambda_3 \left(N_0 + \widehat{I}_{k,m,l} \right) \Psi_{k,m,l}(t)}{(\gamma + \lambda_1) G_{k,m,l} \xi} \right) \right]^+ \quad (35)$$

$$\Psi_{k,m,l}(t+1) = \left[\frac{(1 - \lambda_2) B e^{\widehat{P}_{k,m,l}(t)} G_{k,m,l}}{\ln 2 \cdot \lambda_3 L \left(N_0 + \widehat{I}_{k,m,l} \right)} - 1 \right]^+ \quad (36)$$

Variables λ_1, λ_2 and λ_3 of the dual function in the $(t+1)$-th iteration can be updated by the following update equation, using sub-gradient algorithm in convex optimization as

$$\lambda_1(t+1)$$

$$= \left[\lambda_1(t) + \alpha_1(t) \left(\sum_{k=1}^{K} \sum_{m=1}^{M} \sum_{l=1}^{L} \left(\xi e^{\widehat{P}^*_{k,m,l}} + P_c \right) \right. \right.$$

$$\left. \left. - P_{tot}^{\max} \right) \right]^+ \quad (37)$$

$$\lambda_2(t+1)$$

$$= \left[\lambda_2(t) + \alpha_2(t) \left(\sum_{m=1}^{M} \sum_{l=1}^{L} \frac{B}{L} \right. \right.$$

$$\left. \left. \log_2 \left(1 + \Psi^*_{k,m,l} \right) - \frac{2\left(T_k^{\text{th}} - \overline{X_k}\right)}{2\left(T_k^{\text{th}} - \overline{X_k}\right)\overline{X_k} + \overline{X_k^2}} \right) \right]^+ \quad (38)$$

$$\lambda_3(t+1)$$

$$= \left[\lambda_3(t) + \alpha_3(t) \left(\Psi^*_{k,m,l} e^{-\widehat{P}^*_{k,m,l}} \frac{N_0 + \widehat{I}_{k,m,l}}{G_{k,m,l}} - 1 \right) \right]^+ \quad (39)$$

where α_1, α_2, and α_3 are positive step sizes.

The pseudocode of the SEEPA algorithm given in this paper is shown in Algorithm 2. We first initialize γ, δ, λ_1, λ_2, λ_3, *Ite1*, and *Ite2*. For given values of γ, λ_1, λ_2, and λ_3, $\widehat{P}_{k,m,l}$

Algorithm 2 Sub-Optimal Energy-Efficient Power Allocation

1	Initialize γ, δ and *Ite*1
2	**Repeat**
3	Initialize λ_1, λ_2, λ_3 and *Ite*2
4	**Repeat**
5	Update $\Psi_{k,m,l}$ using equation (35)
6	Update $\widehat{P}_{k,m,l}$ using equation (36)
7	Update λ_1 using equation (37)
8	Update λ_2 using equation (38)
9	Update λ_3 using equation (39)
10	*Ite*2←*Ite*2+1
11	**Until convergence of inner loop**
12	Update γ using equation (30)
13	*Ite*1←*Ite*1+1
14	**Until** $G_{Ite1} < \delta$ **or** *Ite*1= *Ite*1$_{max}$

and $\Psi_{k,m,l}$ are updated through (35)–(36). Then, λ_1, λ_2, and λ_3 are updated using (37)–(39). γ is updated using (30) when the inner loop converges. The outer loop ends when it satisfies the condition $G_{Ite1} < \delta$ or reaches the maximum number of iterations.

VII. EXPERIMENTAL TESTING &ANALYSIS

In this section, the numerical results of Monte Carlo simulations [40]–[45] are presented to evaluate the performance of the EEPA and SEEPA given in the previous section using the equal distribution power allocation (EDPA) algorithm and the genetic power allocation (GPA) algorithm. The simulation parameters are shown in Table 2. Two experimental scenarios were considered: a low-density scenario with 400 users and a high-density scenario with 800 users. In a given scenario, a multi-user spectrum-sharing CR network consisted of a PBS, four SBSs, and the corresponding number of users [43], [46]–[49]. The size of the network was 300 m × 300 m. The number of SBSs was $K = 4$. The PBS was located at (150,150) while the SBSs were located at (75,75), (75,225), (225,75), and (225,225). Because of the small coverage of the SBSs, the height of the antenna of the SBSs could not be ignored. Thus, the height of the antenna of the PBS was set to 50 m and those of the SBSs to 30 m. The average height of the SUs was set to 1.5 m. The topological figures of the multi-user spectrum-sharing CR network are shown in figure 2 and figure 3, where the former shows the low-density scenario with 400 users and the latter the high-density scenario with 800 users [50]–[58]. In figure 2 and figure 3, the red stars denote the SUs and the blue stars the PUs. The total bandwidth $B = 240$ kHz, number of sub-carriers $L = 16$, power consumption of the circuit $P_c = 0.5$W, reciprocal of the drain efficiency of the power amplifier $\xi = 3.8$, and the interference weight vector $V = \left[823 \times 10^{-3}, 88.1 \times 10^{-3}\right]$.

The channel gain of the system was set to Cost 231 Walfish Ikegami model [35]. $G_{k,m,l} = 10^{-\phi(d)/10}$, where $\phi(d) = \phi_{fsl}(d) + \phi_{rts} + \phi_{msd}(d)$ denotes the path loss model between

TABLE 2. Simulation parameters.

Simulation parameters	Values
Total number of users in low-density scenario	400
Total number of users in high-density scenario	800
Number of SBS K	4
Antenna height of PBS	50 m
Antenna height of SBS	30 m
Average height of SU	1.5 m
Total bandwidth B	240 kHz
Number of sub-carriers L	16
Reciprocal of drain efficiency of power amplifier ξ	3.8
Power consumption of circuit P_c	0.5 W
Interference-weighted vector V	$[823 \times 10^{-3}, 88.1 \times 10^{-3}]$
Power spectral density of thermal noise	-174 dBm/Hz
Total power consumption limit P_{tot}^{max}	3×10^3 W
Interference temperature limit	10^{-10}
BER limit	10^{-4}
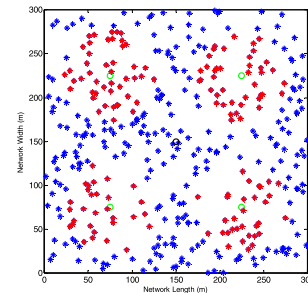
FIGURE 2. Topological model of low-density network of 400 and 800 users scenario.

SU and SBS, ϕ_{fsl} (d) denotes free space loss, ϕ_{rts} denotes the diffraction and scattering losses between the roof and the streets, ϕ_{msd} (d) denotes Multipath loss, and d denotes the distance between SU and SBS. The power spectral density of thermal noise was -174dBm/Hz, the total power constraint was $P_{tot}^{max} = 3 \times 10^3 W$, the interference temperature limit was 10^{-10}, the BER of the system should have been under 10^{-4}, and the maximum delay constraint in the queue was $T_k^{th} = 1$s.

The relationship between the energy efficiency and number of iterations is shown in the figure 4, where F4-A and F4-E represent the EEPA, F4-B and F4-F represent the SEEPA,
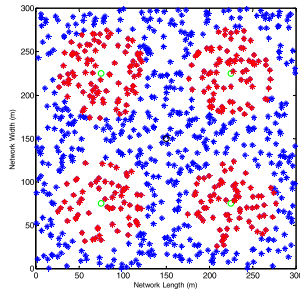
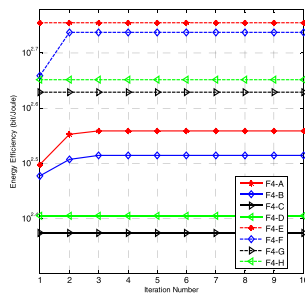**FIGURE 3.** Topological model of low-density network of 400 and 800 users scenario.

FIGURE 4. Relationship between energy efficiency and number of iterations.

F4-C and F4-G represent the EDPA, and F4-D and F4-H represent the GPA. F4-A, F4-B, F4-C, and F4-D represent the low-density scenario while F4-E, F4-F, F4-G, and F4-H represent the high-density scenario. With an increase in the total number of users in the network, the total energy efficiency worsened. In the same scenario, the performance of the EEPA was optimal followed by the SEEPA. The performance of the EDPA and GPA was poor. For the same algorithm, the total energy efficiency in the low-density scenario was better than that in the high-density scenario. Both the EEPA and the SEEPA algorithms designed in this paper converged quickly.
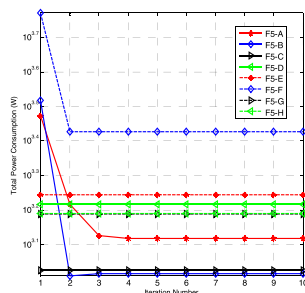
FIGURE 5. Variation in total power consumption with number of iterations.

Figure 5 shows that the total power consumption varied as the number of iteration increased. In contrast with the GPA, the total power consumption of the other three algorithms in the high-density scenario was greater than that in the low-density scenario. Focusing on power allocation in each SU, figures 6 and figure 7 show the relationship between
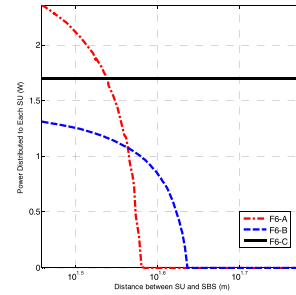
FIGURE 6. Variation in energy efficiency with distances between SUs and SBS in high-density scenario.
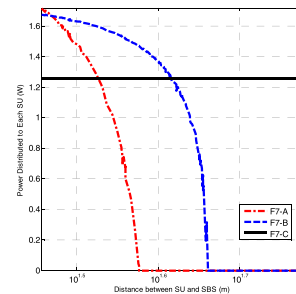

FIGURE 7. Variation in energy efficiency with distances between SUs and SBS in high-density scenario.

the power distributed to each SU and the distance between the SU and the SBS, where the distance between them was the independent variable. F6-A, F6-B, and F6-C show that the power distributed to each SU varied as the distance between SU and SBS increased in the EEPA, SEEPA, and EDPA, separately in the low-density scenario. F7-A, F7-B, and F7-C represent those in the high-density scenario. As shown in the figure, the EDPA distributed equal power to all SUs at different distances from the SBS, whereas the EEPA and SEEPA distributed power only to SUs at 38 m and 45 m from the SBS, respectively. The closer they were to the SBS, the more power was distributed to the SUs. The channel states of SUs far from the SBS were poor. Thus, no power was distributed to them.

In contrast to the power–distance relation in figures 6 and figure 7, figures 8 and figure 9 show the variation in energy efficiency as the distance between SU and SBS increased. F8-A, F8-B, and F8-C represent the variations in the EEPA, SEEPA, and EDPA in the low-density scenario, respectively, whereas F9-A, F9-B, and F9-C represent those in the high-density scenario, respectively. As the distance between SU and SBS increased, the power consumed in link transmission increased while the allocated power to the SU decreased. Then, the energy efficiency of the SU decreased. Under the EDPA scheme, SUs closer to the SBS were assigned the same power as those far from it, so that the energy efficiency of SUs closer to the SBS was much higher than that of those far from it. On the contrary, the power allocation in the EEPA and SEEPA was more reasonable. SUs closer to the SBS were distributed with more power while the energy consumption of those was relatively greater. SUs far from the SBS were
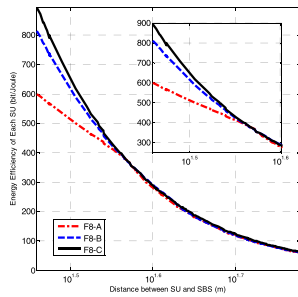
FIGURE 8. Variation in energy efficiency with distances between SUs and SBS in low-density scenario.
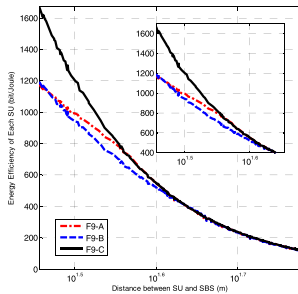

FIGURE 9. Variation in power allocated to each SU with distances between SUs and SBS in high-density scenario.

distributed less power, and even no power, to reduce energy consumption. The energy efficiency of SUs distributed no power was the same in any power allocation method. Thus, it doesn't have practical significance of the EDPA algorithm for allocating power to those SUs.
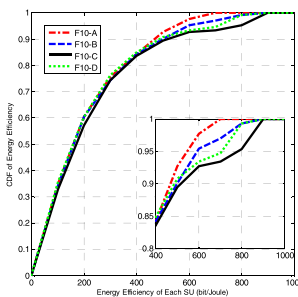

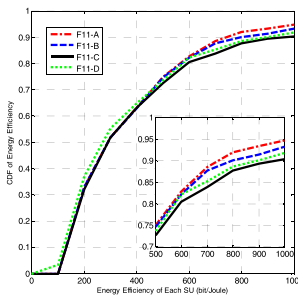**FIGURE 10.** CDF of energy efficiency of each SU in low-density scenario.

FIGURE 11. CDF of energy efficiency of each SU in high-density scenario.

Figures 10 and figure 11 show the cumulative distribution function (CDF) of the energy efficiency of each SU, where F10-A and F11-A represent the EEPA, F10-B and F11-B

represent the SEEPA, F10-C and F11-C represent the EDPA, and F10-D and F11-D represent the GPA. According to the different energy efficiency values, this function indicates the frequency of the energy efficiency of each SU greater than or equal to them. The lowest EDPA curve indicates that more SUs were assigned inappropriate power, leading to lower energy efficiency, whereas the distribution of the EEPA was more reasonable, and it assigned more suitable power to the SUs.

Based on our experiments, when we increase the number of sub-carriers L, we find that the impact of higher number of L on the system's performance is similar to the aforementioned figures, so we ignore the relative redundant figures in order to avoid cumbersome descriptions.

We have analyzed the computation complexity of our method according to the strategy of [55] and [56]. Our method has embedded the computation equation (27), equation (30), or equation (35), or equation (36), and so on, the time complexity is mainly decided by the types of the equations. Based on our analysis, we know that the computation complexity is $O(n)$, and the worst time complexity is $O(n^2)$. So the computation complexity of our method is feasible for the application of the power allocation with limited cross-tier interference for cognitive radio network.

VIII. CONCLUSIONS

A kind of novel method of power allocation with limited cross-tier interference for cognitive radio network is proposed in this paper. To improve the energy efficiency of the entire network, a cross-tier interference limit was presented to protect SUs in the network from too much interference, and a virtual queue was adopted to transform the extra packet delay caused by the contention for channels by multiple users into queuing delay. Taking energy efficiency as the objective function, a nonlinear programming problem with nonlinear constraints was proposed under the constraints of delay and transmission power. The original problem was transformed into a convex polynomial nonlinear programming problem, and the dual Lagrange method was used to determine the global optimal solution. An optimal power allocation algorithm called the EEPA and a sub-optimal power allocation algorithm called the SEEPA were put forward. Experimental comparisons of the EEPA, SEEPA, EDPA, and GPA showed that the EEPA delivers the best performance and improves energy efficiency, and the power allocation to each SU was more reasonable. The SEEPA reduced computational complexity while losing in terms of some aspects of performance. It is thus suitable for many scenarios. In future work, we will focus on the dynamic network model and consider joint resource allocation.

REFERENCES

[1] Q. Zhao and B. M. Sadler, "A survey of dynamic spectrum access," *IEEE Signal Process. Mag.*, vol. 24, no. 3, pp. 79–89, May 2007.

[2] T. Weiss and F. Jondral, "Spectrum pooling: An innovative strategy for the enhancement of spectrum efficiency," *IEEE Commun. Mag.*, vol. 42, no. 3, pp. 8–14, Mar. 2004.

[3] B. Farhang-Boroujeny, "OFDM versus filter bank multicarrier," *IEEE Signal Process. Mag.*, vol. 28, no. 3, pp. 92–112, May 2011.

[4] Y. Medjahdi, M. Terre, D. Le Ruyet, D. Roviras, and A. Dziri, "Performance analysis in the downlink of asynchronous OFDM/FBMC based multi-cellular networks," *IEEE Trans. Wireless Commun.*, vol. 10, no. 8, pp. 2630–2639, Aug. 2011.

[5] G. Y. Li, Z. Xu, C. Xiong, C. Yang, S. Zhang, Y. Chen, and S. Xu, "Energy-efficient wireless communications: Tutorial, survey, and open issues," *IEEE Trans. Wireless Commun.*, vol. 18, no. 6, pp. 29–35, Dec. 2011.

[6] S. Liu, "Novel unequal clustering routing protocol considering energy balancing based on network partition & Distance for mobile education," *J. Netw. Comput. Appl.*, vol. 88, no. 15, pp. 1–9, 2017. doi: 10.1016/j.jnca.2017.03.025.

[7] Y. Chen, S. Zhang, S. Xu, and G. Y. Li, "Fundamental trade-offs on green wireless networks," *IEEE Commun. Mag.*, vol. 49, no. 6, pp. 30–37, Jun. 2011.

[8] D. C. Oh, H. C. Lee, and Y. H. Lee, "Power control and beamforming for femtocells in the presence of channel uncertainty," *IEEE Trans. Veh. Technol.*, vol. 60, no. 6, pp. 2545–2554, Jul. 2011.

[9] J. Zhang, Z. Zhang, and K. Wu, "Optimal distributed subchannel, rate and power allocation algorithm in OFDM-based two-tier femtocell networks," in *Proc. IEEE VTC*, May 2010, vol. 1, no. 1, pp. 1–5.

[10] J. W. Huang and V. Krishnamurthy, "Cognitive base stations in LTE/3GPP femtocells: A correlated equilibrium game-theoretic approach," *IEEE Trans. Commun.*, vol. 59, no. 12, pp. 3485–3493, Dec. 2011.

[11] J. Kim and D.-H. Cho, "A joint power and subchannel allocation scheme maximizing system capacity in indoor dense mobile communication systems," *IEEE Trans. Veh. Technol.*, vol. 59, no. 9, pp. 4340–4353, Nov. 2010.

[12] W. Dang, M. Tao, H. Mu, and J. Huang, "Subcarrier-pair based resource allocation for cooperative multi-relay OFDM systems," *IEEE Trans. Wireless Commun.*, vol. 9, no. 5, pp. 164–1640, May 2010.

[13] C.-N. Hsu, H.-J. Su, and P.-H. Lin, "Joint subcarrier pairing and power allocation for OFDM transmission with decode-and-forward relaying," *IEEE Trans. Singal Process.*, vol. 59, no. 1, pp. 399–414, Jan. 2011.

[14] G. A. S. Sidhu, F. Gao, W. Chen, and A. Nallanathan, "A joint resource allocation scheme for multiuser two-way relay networks," *IEEE Trans. Commun.*, vol. 59, no. 11, pp. 2970–2975, Nov. 2011.

[15] X. Zhang, X. S. Shen, and L. L. Xie, "Joint subcarrier and power allocation for cooperative communications in LTE-advanced networks," *IEEE Trans. Wireless Commun.*, vol. 13, no. 2, pp. 658–668, Feb. 2014.

[16] X. Xiang, C. Lin, and X. Chen, "Toward optimal admission control and resource allocation for LTE-A femtocell uplink," *IEEE Trans. Veh. Technol.*, vol. 64, no. 7, pp. 3247–3261, Jul. 2015.

[17] J. Li, "Delay aware cell association and user scheduling in heterogeneous overlay networks," in *Proc. IEEE PIMRC*, Sep. 2013, vol. 1, no. 1, pp. 106–110.

[18] X. Zhu, B. Yang, C. Chen, L. Xue, X. Guan, and F. Wu, "Cross-layer scheduling for OFDMA-based cognitive radio systems with delay and security constraints," *IEEE Trans. Veh. Technol.*, vol. 64, no. 12, pp. 5919–5934, Dec. 2015.

[19] Y. Guo and Q. Yang, "Cross-layer rate control and resource allocation in spectrum-sharing OFDMA small-cell networks with delay constraints," *IEEE Trans. Veh. Technol.*, vol. 66, no. 5, pp. 4133–4147, May 2017.

[20] C. Jiang, Y. Chen, Y. Gao, and K. J. R. Liu, "Joint spectrum sensing and access evolutionary game in cognitive radio networks," *IEEE Trans. Wireless Commun.*, vol. 12, no. 5, pp. 2470–2483, May 2013.

[21] C. Jiang, Y. Chen, Y. Chen, K. J. R. Liu, and Y. Ren, "Renewal-theoretical dynamic spectrum access in cognitive radio network with unknown primary behavior," *IEEE J. Sel. Areas Commun.*, vol. 31, no. 3, pp. 406–416, Mar. 2013.

[22] D. T. Ngo and T. Le-Ngoc, "Distributed resource allocation for cognitive radio networks with spectrum-sharing constraints," *IEEE Trans. Veh. Technol.*, vol. 60, no. 7, pp. 3436–3449, Sep. 2011.

[23] K. W. Choi, E. Hossain, and D. I. Kim, "Downlink subchannel and power allocation in multi-cell OFDMA cognitive radio networks," *IEEE Trans. Wireless Commun.*, vol. 10, no. 7, pp. 2259–2271, Jul. 2011.

[24] Y. Ma, D. I. Kim, and Z. Wu, "Optimization of OFDMA-based cellular cognitive radio networks," *IEEE Trans. Commun.*, vol. 58, no. 8, pp. 2265–2276, Aug. 2010.

[25] H. Zhang, C. Jiang, N. C. Beaulieu, X. Chu, X. Wen, and M. Tao, "Resource allocation in spectrum-sharing OFDMA femtocells with heterogeneous services," *IEEE Trans. Commun.*, vol. 62, no. 7, pp. 2366–2377, Jul. 2014.

[26] J. H. Yun and K. C. Shin, "Adaptive interference management of OFDMA femtocells for co-channel deployment," *IEEE J. Sel. Areas Commun.*, vol. 29, no. 6, pp. 1225–1241, Jun. 2011.

[27] W. Jing, Z. Lu, H. Zhang, Z. Zhang, J. Zhao, and X. Wen, "Energy-saving resource allocation scheme with QoS provisioning in OFDMA femtocell networks," in *Proc. IEEE ICC*, Jun. 2014, vol. 1, no. 1, pp. 912–917.

[28] H. Zhang, D. Le Ruyet, D. Roviras, and H. Sun, "Uplink capacity comparison of OFDM/FBMC based cognitive radio networks," in *Proc. IEEE Int. Conf. Commun. (ICC)*, May 2010, vol. 1, no. 1, pp. 1–5.

[29] M. Shaat and F. Bader, "A two-step resource allocation algorithm in multicarrier based cognitive radio systems," in *Proc. IEEE Wireless Commun. Netw. Conf. (WCNC)*, Apr. 2010, vol. 1, no. 1, pp. 1–6.

[30] G. Gur and F. Alagoz, "Green wireless communications via cognitive dimension: An overview," *IEEE Netw.*, vol. 25, no. 2, pp. 50–56, Mar./Apr. 2011.

[31] W. Li, J. Lei, T. Wang, C. Xiong, and J. Wei, "Dynamic optimization for resource allocation in relay-aided OFDMA systems under multiservice," *IEEE Trans. Veh. Technol.*, vol. 65, no. 3, pp. 1303–1313, Mar. 2016.

[32] C. C. Zarakovitis and Q. Ni, "Maximizing energy efficiency in multiuser multicarrier broadband wireless systems: Convex relaxation and global optimization techniques," *IEEE Trans. Veh. Technol.*, vol. 65, no. 7, pp. 5275–5286, Jul. 2016.

[33] K. Singh, M. L. Ku, and J.-C. Lin, "Power control for achieving energy-efficient multiuser two-way balancing relay networks," in *Proc. IEEE ICASSP*, May 2014, vol. 1, no. 1, pp. 2749–2753.

[34] K. Singh, A. Gupta, and T. Ratnarajah, "Energy efficient resource allocation for multiuser relay networks," *IEEE Trans. Wireless Commun.*, vol. 16, no. 2, pp. 1218–1235, Feb. 2017.

[35] J. Denis, M. Pischella, and D. Le Ruyet, "Optimal energy-efficient power allocation for asynchronous cognitive radio networks using FBMC/OFDM," in *Proc. IEEE Wireless Conf. Netw. Conf. (WCNC) Track 1: PHY Fundam.*, Apr. 2016, vol. 1, no. 1, pp. 78–85.

[36] S. Liu, D.-G. Zhang, X.-H. Liu, T. Zhang, J.-X. Gao, C.-L. Gong, and Y.-Y. Cui, "Dynamic analysis for the average shortest path length of mobile ad hoc networks under random failure scenarios," *IEEE Access*, vol. 7, pp. 21343–21358, 2019. doi: 10.1109/ACCESS.2019.2896699.

[37] S. Liu and X. H. Liu, "Novel dynamic source routing protocol (DSR) based on genetic algorithm-bacterial foraging optimization (GA-BFO)," *Int. J. Commun. Syst.*, vol. 31, no. 18, pp. 1–20, 2018. doi: 10.1002/dac.3824.

[38] D.-G. Zhang, K. Zheng, D.-X. Zhao, X.-D. Song, and X. Wang, "Novel quick start (QS) method for optimization of TCP," *Wireless Netw.*, vol. 22, no. 1, pp. 211–222, Jan. 2016.

[39] D.-G. Zhang, H.-L. Niu, and S. Liu, "Novel PEECR-based clustering routing approach," *Soft Comput.*, vol. 21, no. 24, pp. 7313–7323, Dec. 2017.

[40] T. Zhang, T. Zhang, and X. Liu, "Novel self-adaptive routing service algorithm for application in VANET," *Appl. Intell.*, vol. 49, no. 5, pp. 1866–1879, 2019. doi: 10.1007/s10489-018-1368-y.

[41] D.-G. Zhang, X. Wang, X.-D. Song, T. Zhang, and Y.-N. Zhu, "A new clustering routing method based on PECE for WSN," *EURASIP J. Wireless Commun. Netw.*, vol. 2015, p. 162, Dec. 2015. doi: 10.1186/s13638-015-0399-x.

[42] T. Zhang and J. Zhang, "A kind of effective data aggregating method based on compressive sensing for wireless sensor network," *J. Wireless Commun. Netw.*, vol. 89, no. 159, pp. 1–15, Dec. 2018. doi: 10.1186/s13638-018-1176-4.

[43] D.-G. Zhang, X. Song, X. Wang, K. Li, W. Li, and Z. Ma, "New agent-based proactive migration method and system for big data environment (BDE)," *Eng. Comput.*, vol. 32, no. 8, pp. 2443–2466, Nov. 2015.

[44] D. Zhang, H. Ge, T. Zhang, Y.-Y. Cui, X. Liu, and G. Mao, "New multi-hop clustering algorithm for vehicular ad hoc networks," *IEEE Trans. Intell. Transp. Syst.*, vol. 20, no. 4, pp. 1517–1530, Apr. 2019. doi: 10.1109/TITS.2018.2853165.

[45] D.-G. Zhang, H.-L. Niu, S. S. Liu, and X.-C. Ming, "Novel positioning service computing method for WSN," *Wireless Pers. Commun.*, vol. 92, no. 4, pp. 1747–1769, Feb. 2017.

[46] Z. Ma, D.-G. Zhang, S. Liu, J. Song, and Y. Hou, "A novel compressive sensing method based on SVD sparse random measurement matrix in wireless sensor network," *Eng. Comput.*, vol. 33, no. 8, pp. 2448–2462, Nov. 2016.

[47] D.-G. Zhang, X. Wang, X. Song, and D. Zhao, "A novel approach to mapped correlation of ID for RFID anti-collision," *IEEE Trans. Services Comput.*, vol. 7, no. 4, pp. 741–748, Oct. 2014.

[48] D.-G. Zhang, S. Zhou, and Y.-M. Tang, "A low duty cycle efficient MAC protocol based on self-adaption and predictive strategy," *Mobile Netw. Appl.*, vol. 23, no. 4, pp. 828–839, May 2017.

[49] Z. Ma, D.-G. Zhang, J. Chen, and Y.-X. Hou, "Shadow detection of moving objects based on multisource information in Internet of Things," *J. Exp. Theor. Artif. Intell.*, vol. 29, no. 3, pp. 649–661, Jul. 2016.

[50] D. Zhang, G. Li, X. Ming, Z.-H. Pan, and K. Zheng, "An energy-balanced routing method based on forward-aware factor for wireless sensor network," *IEEE Trans. Ind. Informat.*, vol. 10, no. 1, pp. 766–773, Feb. 2014.

[51] D.-G. Zhang, K. Zheng, T. Zhang, and X. Wang, "A novel multicast routing method with minimum transmission for WSN of cloud computing service," *Soft Comput.*, vol. 19, no. 7, pp. 1817–1827, Jul. 2015.

[52] T. Zhang, T. Zhang, Y. Dong, X.-H. Liu, Y.-Y. Cui, and D.-X. Zhao, "Novel optimized link state routing protocol based on quantum genetic strategy for mobile learning," *J. Netw. Comput. Appl.*, vol. 122, pp. 37–49, Nov. 2018.

[53] C. Chen, Y. Y. Cui, and T. Zhang, "New method of energy efficient subcarrier allocation based on evolutionary game theory," *Mobile Netw. Appl.*, vol. 24, no. 7, pp. 1–14, Jul. 2018. doi: 10.1007/s11036-018-1123-y.

[54] D.-G. Zhang, "Novel reliable routing method for engineering of Internet of vehicles based on graph theory," *Eng. Comput.*, vol. 36, no. 1, pp. 226–247, 2019. doi: 10.1108/EC-07-2018-0299.

[55] K. Singh, A. Gupta, and T. A. Ratnarajah, "General approach toward green resource allocation in relay-assisted multiuser communication networks," *IEEE Trans. Wireless Commun.*, vol. 17, no. 2, pp. 848–862, Feb. 2018.

[56] K. Singh, A. Gupta, and T. Ratnarajah, "QoS-driven energy-efficient resource allocation in multiuser amplify-and-forward relay networks," *IEEE Trans. Signal Inf. Process. Over Netw.*, vol. 3, no. 4, pp. 771–786, Dec. 2017.

[57] W. Zhang, W. Liu, T. Wang, A. Liu, Z. Zeng, H. Song, and S. Zhang, "Adaption resizing communication buffer to maximize lifetime and reduce delay for WVSNs," *IEEE Access*, vol. 7, pp. 48266–48287, 2019.

[58] J. Li, W. Liu, T. Wang, H. Song, X. Li, F. Liu, and A. Liu, "Battery-friendly based relay selection scheme to prolong lifetime for sensor nodes in Internet of Things," *IEEE Access*, vol. 7, no. 1, pp. 33180–33201, 2019.

JIANNING QIU (M'08) was born in 1981. He is currently pursuing the Ph.D. degree. He is currently a Researcher with the Tianjin University of Technology, Tianjin, China. His research interests include WSN and mobile computing.

XIAODAN ZHANG (M'05) was born in 1972. She received the Ph.D. degree. She is currently a Researcher with the Institute of Institute of Scientific and Technical Information of China, Beijing, China. Her research interests include the IoT and mobile computing.
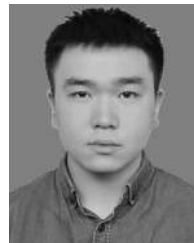
PENGZHEN ZHAO (M'16) was born in 1994. He is currently pursuing the Ph.D. degree. He is currently a Researcher with the Tianjin University of Technology, Tianjin, China. His research interests include WSN and mobile computing.

TING ZHANG (M'05) was born in 1973. She received the Ph.D. degree. She is currently a Researcher with the School of Computer Science and Technology, Tianjin University of Technology, Tianjin, China. Her research interests include the IoT and mobile computing.

DEGAN ZHANG (M'02) was born in 1969. He received the Ph.D. degree from Northeastern University, China. He is currently a Professor with the School of Computer Science and Technology, Tianjin University of Technology, Tianjin, China. His research interests include the IoT, WSN, CRN, and service computing.

CHANGLE GONG (M'16) was born in 1994. He is currently pursuing the Ph.D. degree. He is currently a Researcher with the Tianjin University of Technology, Tianjin, China. His research interests include WSN and mobile computing.

• • •